Highlights on Spanish Astrophysics X, Proceedings of the XIII Scientific Meeting of the Spanish Astronomical Society held on July 16 – 20, 2018, in Salamanca, Spain. B. Montesinos, A. Asensio Ramos, F. Buitrago, R. Schödel, E. Villaver, S. Pérez-Hoyos, I. Ordóñez-Etxeberria (eds.), 2019

Spatially-resolved color–mass-to-light ratio relations in the CALIFA survey.

R. García-Benito[1], R. M. González Delgado[1], E. Pérez[1], R. Cid Fernandes[2], S. F. Sánchez[3], and A. L. de Amorim[2],

[1] Instituto de Astrofísica de Andalucía (CSIC), P.O. Box 3004, 18080 Granada, Spain
[2] Departamento de Física, Universidade Federal de Santa Catarina, P.O. Box 476, 88040-900, Florianópolis, SC, Brazil
[3] Instituto de Astronomía, Universidad Nacional Autónoma de México, Circuito Exterior, Ciudad Universitaria, Ciudad de México 04510, México

Abstract

We calculate the mass-to-light versus color relations (MLCRs) derived from the spatially-resolved star formation history (SFH) of a sample of galaxies from the integral field spectroscopy CALIFA survey. Using full spectral fitting methods we derive the stellar mass ($M_\star$) and combine these results with observed and synthetic colors in optical broad bands. We obtain the radial structure of the mass-to-light ratio (M/L) at several bands and study the MLCRs. Our sample covers a wide range of Hubble types, with stellar masses ranging from $M_\star \sim 10^{8.4}$ to 10^{12} M$_\odot$.

1 Introduction

Large surveys have shown that stellar mass ($M_\star$) is a useful parameter to classify galaxies [22, 9], which in turn is correlated with other global galaxy properties like the stellar mass surface density ($\Sigma_\star$) [15]. Spatially resolved data has shown that $\Sigma_\star$ is a fundamental parameter that drives the star formation history (SFH) of galaxies [2], while integral field spectroscopic surveys have found local relations between $\Sigma_\star$ and other local parameters such as gas and stellar metallicity, age or star formation rate [20, 12, 13].

$M_\star$ and $\Sigma_\star$ are key properties of galaxies that cannot be measured directly. Deriving these quantities from observed data involves stellar populations synthesis (SPS) models. The most common methods to obtain the relation between light and mass involve: a) modeling the galaxy spectrum via full spectral fitting [17, 11] or using spectral indices with a library of parametric star formation histories [16], b) model the spectral energy distribution from

optical-NIR broadband photometry [23], or c) obtaining the relation between colors and the mass-to-light ratio at some wavelength:

$$\log M/L_{\lambda_i} = a_{\lambda_i} + b_{\lambda_i} \times (m_{\lambda_j} - m_{\lambda_k}), \quad (1)$$

where the bands λ_i, λ_j, and λ_k may be independent, or $\lambda_i = \lambda_j$ or $\lambda_i = \lambda_k$.

Certainly, the M/L$_\lambda$-color relation (MLCR) is the simplest method to derive $M_\star$, as it relies on photometry in only two bands.

Most previous works obtain MLCRs based on the integrated M/L_λ [3, 10, 14, 18]. However, galaxies have M/L_λ and color gradients, and the MLCRs can be affected by the spatial variations. In this work, we use the full spectral synthesis technique, fitting the spatially resolved optical spectroscopy provided by the CALIFA survey, to obtain the spatially resolved M/L. Optical colors are measured on observed and on synthetic spectra to explore the effect from the emission lines on the colors in the MLCR. Because the CALIFA sample covers all Hubble types, we are able to explore the radial profiles of M/L_λ and their gradient with galaxy morphology, and their effect on the MLCR.

The sample is selected from the final CALIFA data release [21], with a total of 446 galaxies with the COMB setup, the one used in this work. We group the galaxies into seven morphology bins: E (65 galaxies), S0 (54, including S0 and S0a), Sa (70, including Sa and Sab), Sb (75), Sbc (76), Sc (77, including Sc and Scd), and Sd (35, including Sd, Sm, and Irr).

2 Methodology

We obtain the spatially-resolved SFH of each galaxy to derive the stellar mass surface density ($\Sigma_\star$) and $M_\star$. We follow the same methodology as in previous works (e.g. [12, 13, 11]). In short, we use STARLIGHT [7] to fit the spectrum of each individual spaxel (pixelwise) within the isophote level where the average signal-to-noise ratio (S/N) ≥ 3, decomposing the spectra in terms of stellar populations with different ages and metallicities.

We used base CBe, a set of 246 SSPs from [4] models (Charlot & Bruzual 2007; private communication). The metallicity $\log Z_\star/Z_\odot$ covers from -2.3 to $+0.4$, while ages run from 1 Myr to 14 Gyr. The IMF is that of [6]. Dust effects are modeled as a foreground screen with a [5] reddening law with $R_V = 3.1$. The results are then processed through PyCASSO (the Python CALIFA STARLIGHT Synthesis Organizer; [8, 1]) to produce a multi-dimensional dataset of spatially resolved stellar population properties. From them, 2D maps of M$_\star$, stellar extinction (A$_V$), and luminosity, are obtained to derive 2D maps and radial profiles of M/L.

Colors are computed in two alternative ways: a) convolving the CALIFA data cubes with the SDSS g and r and the Johnson B and V filter responses, and b) convolving the synthetic data cubes obtained from the (pixelwise) full spectral fitting with filters SDSS u, g, r, i, z bands and the B, V, R Johnson bands (*Syn* label).

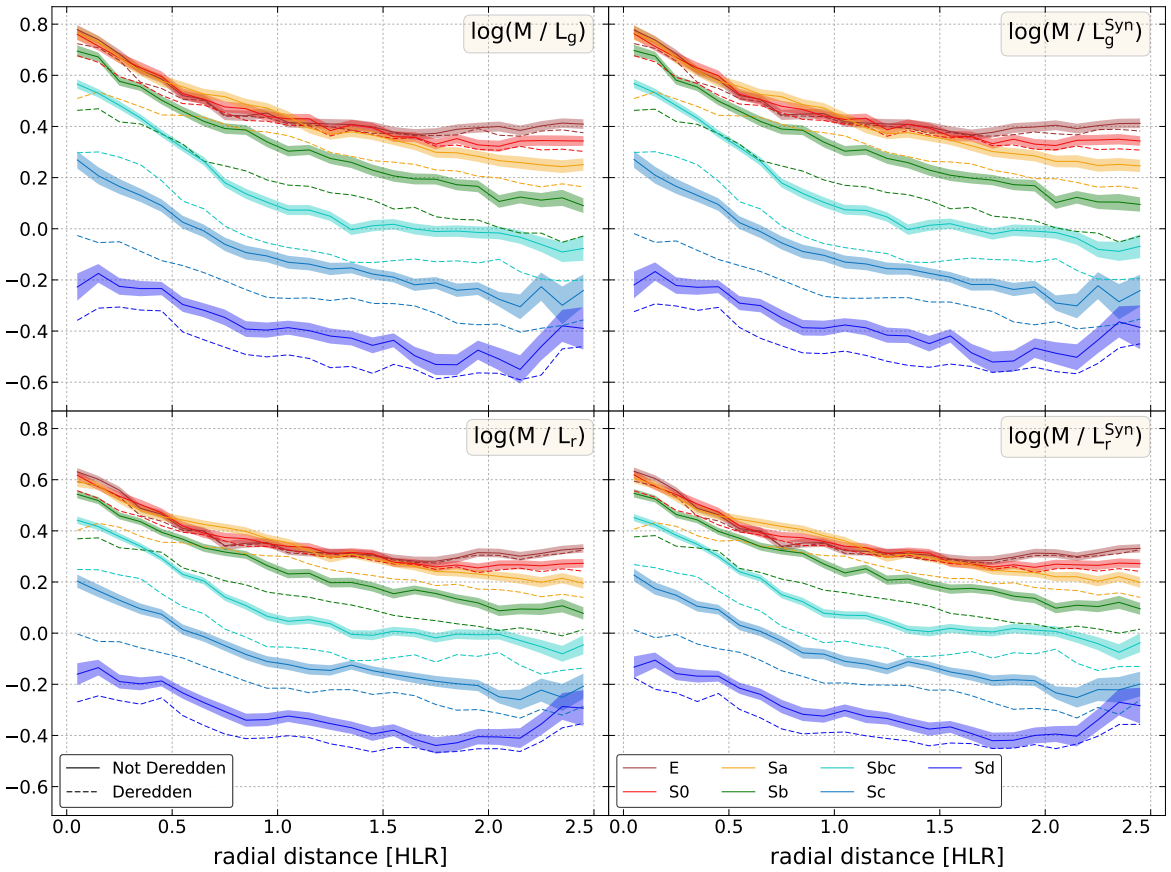

Figure 1: Radial profile of M/L for g band (upper panels) and r band (lower panels) stacked by Hubble type for the observed (left panels) and synthetic restframe spectra (right panels), with intrinsic (continuous lines) and dereddened luminosities (dashed lines).

3 M/L radial profiles

For each galaxy the radial variation of M/L_λ is obtained by compressing each individual 2D map in azimuthally averaged radial profiles. The radial distance is expressed in units of the galaxy's half-light-radius, a convenient metric.

Figure 1 displays azimuthally averaged radial profiles of M/L_g and M/L_r. They have been stacked by Hubble type in seven morphological classes. On the left panels, the profiles are obtained from the observed spectrum, both *not* dereddened (continuous lines) and dereddened (dashed lines). On the right panels we use the M/L images obtained from the synthetic spectra.

All profiles decrease outwards, with inner regions having larger M/L. The profiles scale with the Hubble type. At any given distance, M/L is larger for early type galaxies than for late type spirals. The effect of the extinction is more significant in the central regions of

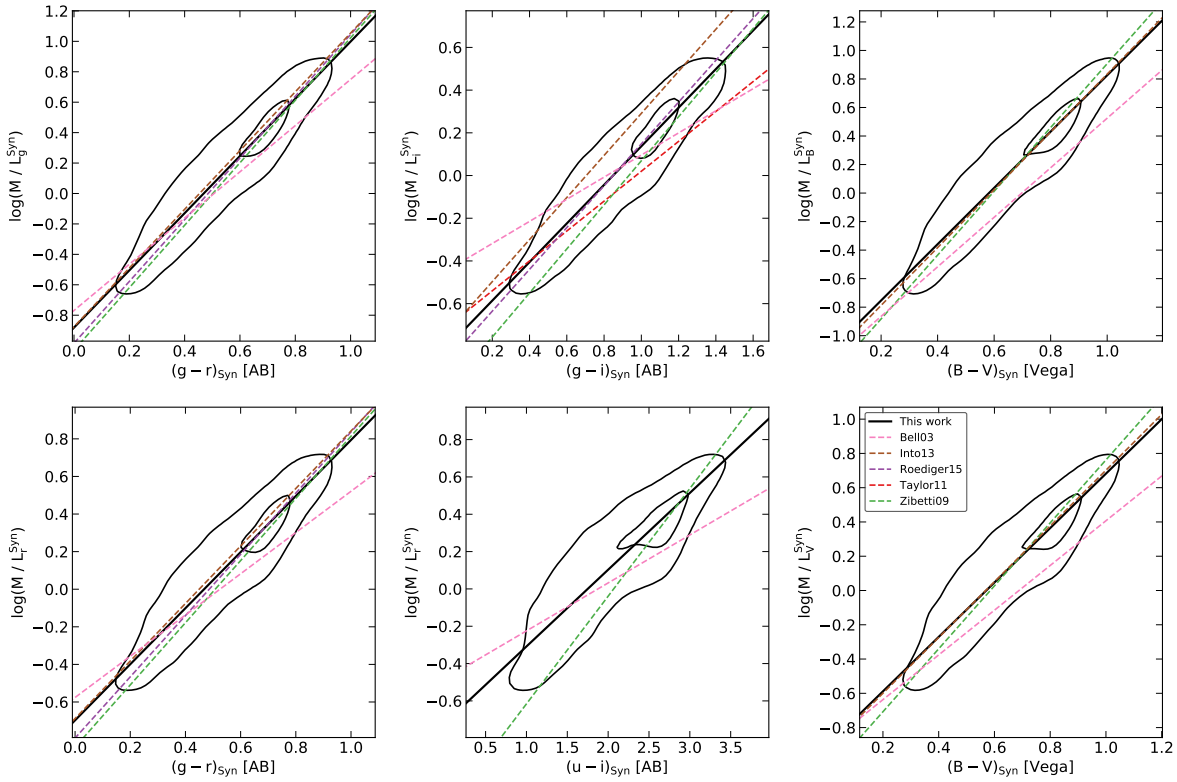

Figure 2: Comparison of the relation between restframe color and M/L for different bands for all galaxies to relations from the literature. The contours represent the density distribution encompassing 90% and 20% of the points.

intermediate type spirals, in particular in Sb/Sbc.

The effect of emission lines is very small, as can be seen from the comparison between observed (left) and synthetic profiles (right). For M/L_g (M/L_r) the maximum difference is around 0.01 dex (0.02 dex) for late type spirals.

4 Spatially-resolved MLCRs

Figure 2 compares a few examples of our empirically calibrated color-log(M/L) relation for different representative bands to other works found in the literature. The (black) contours represent the density distribution of the whole sample encompassing the 90% and 20% of the points. Our spatially resolved MLCRs fits are plotted in solid black lines. All relations have been scaled to our Chabrier IMF.

One of the first linear color-log(M/L) methods was developed by [3], based on on [4] SPS models using dust-free single exponential SFH libraries. As already noticed by later works, the [3] relations present large discrepancies. They strongly deviate towards lower values of M/L, with differences of a few dex in some filters (e.g. $g - i$).

Later works have compiled new MLCRs using different ingredients and methods. For example, [14] disc galaxy models runs very close to ours, except for $g-i$, which overestimates M/L by ~ 0.15 dex as compared to our results.

Relations by [18] and [24] also run close to our values, although the later has some discrepancies in the $M/L_i - (g-i)$, particularly in the $M/L_i - (g-i)$ combination for low M/L ratios.

Finally, the [23] relation, calibrated using SDSS *ugriz* multi-band photometry of a large sample of galaxies, diverges from our relation in the $M/L_i - (g-i)$ plane for medium to large M/L values, i.e. intermediate and early type galaxies.

5 Conclusions

Our results are in agreement with previous results based on integrated M/L and colors of galaxies, with M/L_g and M/L_r being remarkably similar to the results from [24], [14], and [18]. In the plane $M/L_i - (g-i)$ there is more dispersion, but our results are similar to [18] and they are in between [24] and [14] for $(g\text{-}i) < 1$, and [23] and [14] for redder colors. In the plane $M/L_r - (u-i)$ our relation is in between [3] and [24]. In the $M/L_V - (B-V)$ plane, our results are in perfect agreement with [18], and very close to [24]. The relation $M/L_B - (B-V)$ is very tight and all the results, ours included, agree very well, with the exception of [3].

The values of the slope and intercept of the MLCRs for all bands, for the whole sample and with different morphological bins, can be found in our webpage `http://pycasso.iaa.es/ML`.

Acknowledgments

CALIFA is the first legacy survey carried out at Calar Alto. The CALIFA collaboration would like to thank the IAA-CSIC and MPIA-MPG as major partners of the observatory, and CAHA itself, for the unique access to telescope time and support in manpower and infrastructures. We also thank the CAHA staff for the dedication to this project. We thank the support of the IAA Computing group. Support from the Spanish Ministerio de Economía y Competitividad, through projects AYA2016-77846-P, AYA2014-57490-P, AYA2010-15081, and Junta de Andalucía P12-FQM-2828. SFS is grateful for the support of a CONACYT (Mexico) grant CB-285080, and funding from the PAPIIT-DGAPA-IA101217 (UNAM).

References

[1] de Amorim, A. L., García-Benito, R., Cid Fernandes, R., et al. 2017, MNRAS, 471, 3727

[2] Bell, E. F., & de Jong, R. S. 2000, MNRAS, 312, 497

[3] Bell, E. F., McIntosh, D. H., Katz, N., & Weinberg, M. D. 2003, ApJS, 149, 289

[4] Bruzual, G., & Charlot, S. 2003, MNRAS, 344, 1000

[5] Cardelli, J. A., Clayton, G. C., & Mathis, J. S. 1989, ApJ, 345, 245

[6] Chabrier, G. 2003, PASP, 115, 763

[7] Cid Fernandes, R., Mateus, A., Sodré, L., Stasińska, G., & Gomes, J. M. 2005, MNRAS, 358, 363

[8] Cid Fernandes, R., Pérez, E., García Benito, R., et al. 2013, A&A, 557, A86

[9] Driver, S. P., Hill, D. T., Kelvin, L. S., et al. 2011, MNRAS, 413, 971

[10] Gallazzi, A., & Bell, E. F. 2009, ApJS, 185, 253

[11] García-Benito, R., González Delgado, R. M., Pérez, E., et al. 2017, A&A, 608, A27

[12] González Delgado, R. M., Pérez, E., Cid Fernandes, R., et al. 2014, A&A, 562, A47

[13] González Delgado, R. M., Cid Fernandes, R., Pérez, E., et al. 2016, A&A, 590, A44

[14] Into, T., & Portinari, L. 2013, MNRAS, 430, 2715

[15] Kauffmann, G., Heckman, T. M., White, S. D. M., et al. 2003, MNRAS, 341, 54

[16] López Fernández, R., González Delgado, R. M., Pérez, E., et al. 2018, A&A, 615, A27

[17] Panter, B., Heavens, A. F., & Jimenez, R. 2003, MNRAS, 343, 1145

[18] Roediger, J. C., & Courteau, S. 2015, MNRAS, 452, 3209

[19] Sánchez, S. F., Kennicutt, R. C., Gil de Paz, A., et al. 2012, A&A, 538, A8

[20] Sánchez, S. F., Rosales-Ortega, F. F., Jungwiert, B., et al. 2013, A&A, 554, A58

[21] Sánchez, S. F., García-Benito, R., Zibetti, S., et al. 2016, A&A, 594, A36

[22] Stoughton, C., Lupton, R. H., Bernardi, M., et al. 2002, AJ, 123, 485

[23] Taylor, E. N., Hopkins, A. M., Baldry, I. K., et al. 2011, MNRAS, 418, 1587

[24] Zibetti, S., Charlot, S., & Rix, H.-W. 2009, MNRAS, 400, 1181